A logderivative propagation scheme for the exact solution of twostate curve crossing problems

Millard H. Alexander, Gérard Parlant, and Terrence H. Hemmer

Citation: The Journal of Chemical Physics **91**, 2388 (1989); doi: 10.1063/1.456996
View online: http://dx.doi.org/10.1063/1.456996
View Table of Contents: http://scitation.aip.org/content/aip/journal/jcp/91/4?ver=pdfcov
Published by the AIP Publishing

A log-derivative propagation scheme for the exact solution of two-state curve crossing problems

Millard H. Alexander, Gérard Parlant,[a] and Terrence H. Hemmer
Department of Chemistry, University of Maryland, College Park, Maryland 20742

(Received 11 April 1989; accepted 27 April 1989)

A new method is presented for the exact quantum solution of certain two-state curve crossing problems, where electronic state $|1\rangle$ is energetically open at one end of the range of integration, while state $|2\rangle$, and, possibly, state $|1\rangle$, is energetically open at the other end of the range of integration. The method involves the use of log-derivative propagators, but differs from the usual log-derivative integration scheme in that one must propagate through the range of integration not only the log-derivative matrix but also a transformation matrix which permits one to reconstruct the initial wave function after the integration is completed. The method is numerically stable and, in a "solution following" approximation to the log-derivative propagators, converges as the fourth power of the step size. Application is made to several model problems. In one case the exact results are compared with the predictions of earlier semiclassical analyses [P. V. Coveney, M. S. Child, and A. Bárány, J. Phys. B **18**, 457 (1985)]. The method is completely general, and can be applied to arbitrary potentials.

I. INTRODUCTION

Curve crossing between two electronic states is a venerable problem in molecular physics. Three types of situations are often encountered, shown schematically in Fig. 1. Since the early work of Landau and Zener,[1] numerous articles have been devoted to the development of methods for the determination of transition probabilities from one state to the other. Much of this work has been within the framework of time-dependent impact parameter theory.[2–6] In this approach the collision partners are assumed to follow a trajectory which determines the time dependence of the coupling between the two states. Transition probabilities are then determined within a standard time-dependent treatment of the dynamics. Within the past 2 years Metiu and co-workers[7,8] have presented an alternative time-dependent approach based on wave-packet propagation, either exact or within a Gaussian approximation. This work has had direct relevance to the interpretation[9] of recent time-dependent photodissociation experiments[10] in which the time dependence of product formation is mediated by a curve crossing in the exit channel.

In our own group we have become involved in the interpretation[11–13] of the study, by King and co-workers[14] of the decomposition of HN_3 induced by infrared pumping. Here, the lowest energy decomposition channel corresponds to a spin–orbit induced crossing between two potential surfaces. At higher degrees of internal excitation both the spin-allowed and the spin-forbidden channels are open, so that the decomposition process can be represented schematically by the right-hand panel in Fig. 1. In order to model these experiments, which can be described only poorly by classical Rice–Ramsberger–Kassel–Marcus (RRKM) theory,[14] it is necessary to develop a technique to determine the spin-forbidden transition probability and, at higher degrees of excitation, the distribution of the decomposition flux between the spin-allowed and spin-forbidden channels. This is the goal of the present paper. Our aim is the development of a computationally simple, yet accurate method, which can be applied to potentials of any functional form. Thus our objective is somewhat complementary to that of much of the earlier semiclassical work,[1–6] which was aimed at the extraction of analytical formulas for idealized potentials and valid over restricted energy ranges.

There exist a large number of numerical integration techniques[15–33] which can be applied to the solution of the coupled Schrödinger equations which describe any of the two-state curve crossing problems represented schematically in Fig. 1. In practice, the situation represented by the middle panel of Fig. 1 is particularly difficult, since one state is closed at the left-hand side of the range of integration while the other is closed at the right-hand side. Thus, regardless of the direction of propagation, one is obliged to integrate into a classically forbidden region, which will lead to severe problems of numerical stability due to the exponential character of the closed channel components in the wave function.[25] As will be shown here, these problems of numerical stability can be circumvented by use of a log-derivative propagation scheme,[21,25,29–33] a technique due originally to Johnson.[21] The same method can be used regardless of whether one or both states are open asymptotically. Our time-independent approach is complementary to the time-dependent wave-packet propagation technique of Metiu and co-workers.[7,8]

The organization of the present paper is as follows: In the next section we describe the mathematics of our propagation scheme, which is similar to a technique proposed by Mrugala and Secrest[32] for collinear reactive scattering problems. Some aspects of this propagation scheme have already been presented in another context.[34] Then, in Sec. III we apply this technique to an idealized curve crossing created by two intersecting linear potentials, with a constant coupling potential. Here a comparison can be made with the semiclassical results of Coveney, Child, and Bárány.[5] Application to the situation described in the right-hand panel of Fig. 1, where one or both states can be open asymptotically,

[a] Permanent address: PCR (UA 75, associated with the CNRS), Bâtiment 350, Université Paris-Sud, 91405 Orsay cedex, France.

 0021-9606/89/162388-08$02.10

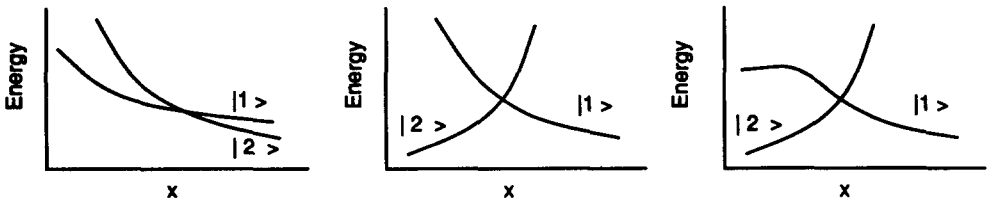

FIG. 1. Schematic diagram of three types of curve crossing situations. In the left-hand panel both states are energetically accessible (open) as the interparticle separation goes to $+\infty$ but become inaccessible (closed) at short distances. In the middle panel one state is open at large positive distances but closed at large negative distances while the other state is closed at large positive distances and open at large negative distances. In the right-hand panel only one state is open at large positive distances while one or two states may be open at large negative distances. Shown here are the diabatic states. The coupling between them may be large or small and may (or may not) depend on the distance. In the case of the middle and right-hand panels, the collision energy may be below or above the crossing point. In the case of the left- and right-hand panels, the collision energy may be above or below the asymptotic (large distance) energy of the higher state.

is made in Sec. IV. Here, we use a set of potentials drawn from our recent *ab initio* potential energy surfaces for the HN_3 molecule.[13] A brief conclusion follows.

II. SOLUTION OF COUPLED EQUATIONS AND DETERMINATION OF TRANSMITTED FLUX

The Schrödinger equation for the general two-state problem is

$$\left[\mathbf{1}\frac{d^2}{dx^2} - \mathbf{W}(x)\right]\mathbf{F}(x) = 0. \tag{1}$$

Here $\mathbf{1}$ designates the identity matrix, x is the interparticle distance, and the matrix $\mathbf{W}(x)$ is given by

$$\mathbf{W}(x) = (2\mu/\hbar^2)[\mathbf{V}(x) - E\mathbf{1}], \tag{2}$$

where μ is the reduced mass of the collision system, E is the total energy, and the matrix $\mathbf{V}(x)$ is the (full, symmetric) matrix of the coupling potential. The two diagonal elements $V_{11}(x)$ and $V_{22}(x)$ are the diabatic potentials of the two states, such as those shown in Fig. 1, while the off-diagonal element $V_{12}(x)$ is the diabatic coupling potential. We shall assume that as $x \to \pm\infty$, the coupling potential goes to zero while the diagonal potential matrix elements go to constant values.

The goal is to propagate numerically the matrix of solutions $\mathbf{F}(x)$. Consider a situation such as that described in the middle or right-hand panels of Fig. 1. Assume that only state $|1\rangle$ is open at the right. At the left, only state $|2\rangle$ will be open at low energy, while at higher energies, state $|1\rangle$ may also be open. Furthermore, assume that we are interested in a system in which flux is incoming from the right, so that as $x \to \infty$ there will be only outgoing flux in state $|2\rangle$. The boundary conditions on the wave function as $x \to \infty$ can be written, if just state $|2\rangle$ is open,

$$\lim_{x\to-\infty}\mathbf{F}(x) = \begin{bmatrix} k_{1l}^{-1/2}\exp(k_{1l}x) & 0 \\ 0 & k_{2l}^{-1/2}\exp(-ik_{2l}x)\end{bmatrix}\mathbf{T}, \tag{3}$$

and, if states $|1\rangle$ and $|2\rangle$ are open,

$$\lim_{x\to-\infty}\mathbf{F}(x) = \begin{bmatrix} k_{1l}^{-1/2}\exp(-ik_{1l}x) & 0 \\ 0 & k_{2l}^{-1/2}\exp(-ik_{2l}x)\end{bmatrix}\mathbf{T}. \tag{4}$$

Here $\mathbf{T}$, the transmission amplitude, is a square constant matrix and the wave vectors $k_{il}(i = 1,2)$, where the subscript l designates "left," are defined by

$$k_{il} = \lim_{x\to-\infty}[2\mu|E - V_{ii}(x)|]^{1/2}/\hbar, \tag{5}$$

where the positive root is implied. As will be shown below, in actual practice the determination of the $\mathbf{T}$ matrix is never necessary.

Asymptotically, as $x \to +\infty$, the wave function can be written in the following general form:

$$\lim_{x\to+\infty}\mathbf{F}(x) = \mathbf{I}_r(x) + \mathbf{O}_r(x)\mathbf{R}, \tag{6}$$

where $\mathbf{R}$ is a constant matrix and the matrices $\mathbf{I}_r(x)$ and $\mathbf{O}_r(x)$, which designate, respectively, incoming and outgoing solutions as $x \to +\infty$, are given by

$$\begin{bmatrix} k_{1r}^{-1/2}\exp(\pm ik_{1r}x) & 0 \\ 0 & k_{2r}^{-1/2}\exp(\pm k_{2r}x)\end{bmatrix}, \tag{7}$$

where the plus sign refers to the $\mathbf{O}_r$ matrix, and the minus sign to the $\mathbf{I}_r$ matrix. Here, similarly to Eq. (5), the wave vectors are defined by

$$k_{ir} = \lim_{x\to\infty}[2\mu|E - V_{ii}(x)|]^{1/2}/\hbar. \tag{8}$$

The two columns of the $\mathbf{F}(x)$ matrix correspond to the two linearly independent solutions to Eq. (1) which obey the correct boundary conditions as $x \to -\infty$. The first column vector is

$$\mathbf{f}(x_{\max}) \equiv \begin{bmatrix} f_1(x_{\max}) \\ f_2(x_{\max})\end{bmatrix} = \begin{bmatrix} k_{1r}^{-1/2}[\exp(-ik_{1r}x_{\max}) + R_{11}\exp(ik_{1r}x_{\max})] \\ k_{2r}^{-1/2}R_{21}\exp(k_{2r}x_{\max})\end{bmatrix}, \tag{9}$$

where x_{max} is a value of the distance sufficiently large that the potential matrix has attained its asymptotic value. Let us define a *flux vector* $\mathbf{j}_r$ associated with the solution $\mathbf{f}(x_{max})$ whose ith element is the flux in state $|i\rangle$ as $x \to +\infty$. In other words,

$$(\mathbf{j}_r)_i = \lim_{x\to\infty} -(i\hbar/2\mu)\left\{f_i(x)\left[\frac{d}{dx}f_i(x)\right]^* + \text{C.C.}\right\}. \tag{10}$$

In the present case we have

$$(\mathbf{j}_r)_1 = -(i\hbar/\mu)(1-|R_{11}|^2), \tag{11a}$$

$$(\mathbf{j}_r)_2 = 0. \tag{11b}$$

Similar to Eq. (10) we can define a flux vector $\mathbf{j}_l$ whose ith element is the flux in state $|i\rangle$ as $x \to -\infty$. If only state $|2\rangle$ is open as $x \to -\infty$ (a situation described by the middle panel of Fig. 1), then

$$(\mathbf{j}_l)_1 = 0, \tag{12a}$$

$$(\mathbf{j}_l)_2 = -(i\hbar/\mu)|T_{21}|^2. \tag{12b}$$

Since current must be conserved, we have

$$|T_{21}|^2 = 1 - |R_{11}|^2. \tag{13}$$

Thus, with the (11) element of the **R** matrix one can fully describe the dynamics of the system; all physically meaningful information is contained in this reflection amplitude R_{11}. The transmission probability, which is just the transition probability from state $|1\rangle$ to state $|2\rangle$, is

$$P_{12} = |T_{21}|^2 = 1 - |R_{11}|^2. \tag{14}$$

In the case where both state $|1\rangle$ and $|2\rangle$ are open as $x \to -\infty$ (a situation described by the right-hand panel of Fig. 1), then the elements of the flux vector $\mathbf{j}_l$ are

$$(\mathbf{j}_l)_i = -(i\hbar/\mu)|T_{i1}|^2. \tag{15}$$

The condition of conservation of current now implies that

$$|T_{11}|^2 + |T_{21}|^2 = 1 - |R_{11}|^2. \tag{16}$$

Now, in order to uniquely specify the physically important scattering information, it appears necessary to determine the magnitude of the elements of the transmission amplitude matrix **T**, or, at least, of the first column of this matrix.

The required information can be obtained by working with the logarithmic derivative of the solution matrix $\mathbf{F}(x)$, namely

$$\mathbf{Y}(x) = \mathbf{F}'(x)\mathbf{F}(x)^{-1}, \tag{17}$$

where the prime designates differentiation with respect to x. From Eqs. (3) and (4) one can show that the log-derivative matrix $\mathbf{Y}(x)$ as $x \to -\infty$ is *independent* of the transmission amplitude matrix **T** and given by

$$\lim_{x\to-\infty} \mathbf{Y}(x) = \begin{bmatrix} k_{1l} & 0 \\ 0 & -ik_{2l} \end{bmatrix}, \tag{18}$$

when only state $|2\rangle$ is open, and by

$$\lim_{x\to-\infty} \mathbf{Y}(x) = \begin{bmatrix} -ik_{1l} & 0 \\ 0 & -ik_{2l} \end{bmatrix}, \tag{19}$$

when both states $|1\rangle$ and $|2\rangle$ are open.

As proposed first by Johnson,[21] with subsequent work by others,[21,29–33] it is possible to propagate numerically the log-derivative matrix directly, obtaining thereby $\mathbf{Y}(+\infty)$ from $\mathbf{Y}(-\infty)$ [Eqs. (18) or (19)]. As we shall show in the next section, one can concurrently obtain the matrix $\mathbf{G}(-\infty,+\infty) \equiv \mathbf{F}(-\infty)\mathbf{F}(+\infty)^{-1}$, which relates the solution matrices at each end of the range of integration. With $\mathbf{G}(-\infty,+\infty)$ and $\mathbf{Y}(+\infty)$ one can obtain the desired flux vectors $\mathbf{j}_r$ [Eq. (11)] and $\mathbf{j}_l$ [Eqs. (12) or (15)] which fully describe the collision, without explicitly determining the transmission amplitude matrix **T**. This is done as follows.

From Eqs. (6) and (7) and the definition of the log-derivative matrix [Eq. (17)] we see that **R** must satisfy the matrix equation

$$\mathbf{Y}(x_{max}) = [\mathbf{I}_r'(x_{max}) + \mathbf{O}_r'(x_{max})\mathbf{R}] \times [\mathbf{I}_r(x_{max}) + \mathbf{O}_r(x_{max})\mathbf{R}]^{-1}. \tag{20}$$

Thus the matrix **R** is given by

$$\mathbf{R} = [\mathbf{Y}(x_{max})\mathbf{O}_r(x_{max}) - \mathbf{O}_r'(x_{max})]^{-1} \times [\mathbf{I}_r'(x_{max}) - \mathbf{Y}(x_{max})\mathbf{I}_r(x_{max})]. \tag{21}$$

From Eq. (21) one determines the constants R_{11} and R_{21} which define the wave function at $x = x_{max}$ [Eq. (9)]. The corresponding wave function at $x = x_{min}$ is given by

$$\mathbf{f}(x_{min}) = \mathbf{G}(x_{min},x_{max})\mathbf{f}(x_{max}) = \mathbf{F}(x_{min})\mathbf{F}(x_{max})^{-1}\mathbf{f}(x_{max}), \tag{22}$$

where x_{min} designates a value of the distance sufficiently large and *negative* that the potential matrix has attained its asymptotic value.

From the definition of the log-derivative matrix [Eq. (17)] the derivative of the wave function at $x = x_{min}$ is given by

$$\mathbf{f}'(x_{min}) = \mathbf{Y}(x_{min})\mathbf{f}(x_{min}). \tag{23}$$

Hence, the elements of the flux vector at x_{min}, $\mathbf{j}_l$ [Eqs. (12) or (15)], are given by, in analogy with Eq. (10),

$$(\mathbf{j}_l)_i = -(i\hbar/2\mu)\{f_i(x_{min})[\mathbf{Y}(x_{min})\mathbf{f}(x_{min})]_i^* + \text{C.C.}\}. \tag{24}$$

The single nonvanishing element of the $\mathbf{j}_r$ flux vector, $(\mathbf{j}_r)_1$, is, we remember, defined by R_{11} [Eq. (11a)]. Thus, as anticipated, one can obtain the physically meaningful scattering formation without explicit determination of the transmission amplitude matrix **T**.

III. DETAILS OF LOG-DERIVATIVE PROPAGATION SCHEME

The implementation of the log-derivative propagation scheme is described below. For more details we refer the reader to the work of Mrugala and Secrest[31,32] and Manolopoulos.[29,33] The integration range ($x_{min} \leqslant x \leqslant x_{max}$) is divided into a number of small intervals. Consider one such interval, defined by two values of the internuclear separation x_a and x_b, with $x_b > x_a$. Within a log-derivative propagation scheme the wave function $\mathbf{F}(x)$ and its derivative at x_a and x_b are related by the matrix equation[31,32,33]

$$\begin{bmatrix}\mathbf{F}'(x_a)\\ \mathbf{F}'(x_b)\end{bmatrix}=\begin{bmatrix}\mathbf{L}_1(a,b) & \mathbf{L}_2(a,b)\\ \mathbf{L}_3(a,b) & \mathbf{L}_4(a,b)\end{bmatrix}\begin{bmatrix}-\mathbf{F}(x_a)\\ \mathbf{F}(x_b)\end{bmatrix}, \tag{25}$$

where the log-derivative propagators $\mathbf{L}_i(a,b)$ are $N\times N$ matrices. From Eq. (25) and the definition of the log-derivative matrix [Eq. (17)] one can show that the log-derivative matrix at x_b can be expressed in terms of the log-derivative matrix at x_a as

$$\mathbf{Y}(x_b)=\mathbf{L}_4(a,b)-\mathbf{L}_3(a,b)[\mathbf{Y}(x_a)+\mathbf{L}_1(a,b)]^{-1}\mathbf{L}_2(a,b). \tag{26}$$

It then follows that

$$\mathbf{G}(x_a,x_b)\equiv\mathbf{F}(x_a)\mathbf{F}(x_b)^{-1}=[\mathbf{Y}(x_a)+\mathbf{L}_1(a,b)]^{-1}\mathbf{L}_2(a,b). \tag{27}$$

By repeated application of Eq. (26) one can propagate the initial log-derivative matrix $\mathbf{Y}(x_{\min})$ to obtain $\mathbf{Y}(x_{\max})$. Simultaneous with propagation of $\mathbf{Y}(x)$ we can construct, by repeated application of Eq. (27), the matrix $\mathbf{G}$ defined immediately prior to Eq. (20). We find

$$\begin{aligned}\mathbf{G}&\equiv\mathbf{F}(x_{\min})\mathbf{F}(x_{\max})^{-1}\\ &=\mathbf{F}(x_{\min})\mathbf{F}(x_a)^{-1}\mathbf{F}(x_a)\mathbf{F}(x_b)^{-1}\mathbf{F}(x_b)\mathbf{F}(x_c)^{-1}\cdots\\ &\quad\times\mathbf{F}(x_y)\mathbf{F}(x_z)^{-1}\mathbf{F}(x_z)\mathbf{F}(x_{\max})^{-1}\\ &=\mathbf{G}(x_{\min},x_a)\mathbf{G}(x_a,x_b)\mathbf{G}(x_b,x_c)\cdots\\ &\quad\times\mathbf{G}(x_y,x_z)\mathbf{G}(x_z,x_{\max}).\end{aligned} \tag{28}$$

The standard implementation of this log-derivative propagation scheme is based on the modified Simpson's rule approximation[31–33] to the log-derivative propagators $\mathbf{L}_i(a,b)$ suggested originally by Johnson.[21] In this approximation the interval between x_a and x_b is divided in half. Let x_m define the midpoint of the interval, with $x_m=(x_a+x_b)/2$. Then propagation of $\mathbf{Y}(x)$ from x_a to x_b is accomplished by first propagating to $x=x_m$, using Eq. (26) and the following half-interval propagators:

$$h\,\mathbf{L}_1(a,m)=h\,\mathbf{L}_1^0(a,m)+(h^2/3)\mathbf{W}_1(x_a), \tag{29a}$$

$$h\,\mathbf{L}_2(a,m)=h\,\mathbf{L}_2^0(a,m), \tag{29b}$$

$$h\,\mathbf{L}_3(a,m)=h\,\mathbf{L}_3^0(a,m), \tag{29c}$$

$$h\,\mathbf{L}_4(a,m)=h\,\mathbf{L}_4^0(a,m)+(2h^2/3)\tilde{\mathbf{W}}_1(x_m). \tag{29d}$$

Here $h=(x_b-x_a)/2$, $\mathbf{W}_1(x)$ is an approximation to the full $\mathbf{W}(x)$ matrix [Eq. (1)], and $\tilde{\mathbf{W}}_1(x_m)$ is given by

$$\tilde{\mathbf{W}}_1(x_m)=(6/h^2)[1-(h^2/6)\mathbf{W}_1(x_m)]^{-1}-(6/h^2)\mathbf{1}. \tag{30}$$

Possible choices of the $\mathbf{W}_1(x)$ matrix will be defined later in this section. Subsequently, propagation of $\mathbf{Y}(x)$ from x_m to x_b is done using Eq. (26) and the following half-interval propagators:

$$h\,\mathbf{L}_1(m,b)=h\,\mathbf{L}_1^0(m,b)+(h^2/3)\tilde{\mathbf{W}}_1(x_m), \tag{31a}$$

$$h\,\mathbf{L}_2(m,b)=h\,\mathbf{L}_2^0(m,b), \tag{31b}$$

$$h\,\mathbf{L}_3(m,b)=h\,\mathbf{L}_3^0(m,b), \tag{31c}$$

$$h\,\mathbf{L}_4(m,b)=h\,\mathbf{L}_4^0(m,b)+(2h^2/3)\mathbf{W}_1(x_b). \tag{31d}$$

Now, since

$$\mathbf{F}(x_a)\mathbf{F}(x_b)^{-1}=\mathbf{F}(x_a)\mathbf{F}(x_m)^{-1}\mathbf{F}(x_m)\mathbf{F}(x_b)^{-1} \tag{32}$$

it follows that

$$\mathbf{G}(x_a,x_b)=\mathbf{G}(x_a,x_m)\mathbf{G}(x_m,x_b). \tag{33}$$

The transformation matrix $\mathbf{G}(x_a,x_b)$ can thus be constructed by using Eq. (27) with the half-interval propagators defined by Eq. (29) to construct first $\mathbf{G}(x_a,x_m)$ and then the half-interval propagators defined by Eq. (31), as well as $\mathbf{Y}(x_m)$—which must be determined during the propagation of the log-derivative matrix—to construct $\mathbf{G}(x_m,x_b)$.

As proven by Manolopoulos,[33] Eqs. (29)–(31) apply for any piecewise continuous diagonal reference potential, provided the homogeneous propagators $\mathbf{L}_i^0$ are constructed accordingly. In the simplest implementation of the log-derivative propagation scheme, due to Johnson,[21] the reference half-interval propagators, $\mathbf{L}_i^0(q,p)$ in Eqs. (29) and (31), multiplied by the half-interval step size h, are equal to a unit matrix, and the potential matrix $\mathbf{W}_1(x)$ is just the $\mathbf{W}(x)$ matrix defined in Eq. (1).[33] Manolopoulos has recently proposed[29,33] a more accurate integration scheme which is based on first partitioning the $\mathbf{W}(x)$ matrix in the interval (a,b) as

$$\mathbf{W}(x)=\mathbf{W}_0+\mathbf{W}_1(x), \tag{34}$$

where $(\mathbf{W}_0)_{ij}=\delta_{ij}W_{ii}(x_m)$, so that

$$[\mathbf{W}_1(x)]_{ij}=[\mathbf{W}(x)]_{ij}-\delta_{ij}W_{ii}(x_m). \tag{35}$$

The reference half-interval propagators are now given by

$$h\,[\mathbf{L}_1^0(a,m)]_{ij}=h\,[\mathbf{L}_4^0(a,m)]_{ij}=\delta_{ij}\begin{cases}|p_i|h\coth|p_i|h, & p_i^2\geqslant 0\\ |p_i|h\cot|p_i|h, & p_i^2\leqslant 0\end{cases} \tag{36}$$

and

$$h\,[\mathbf{L}_2^0(a,m)]_{ij}=h\,[\mathbf{L}_3^0(a,m)]_{ij}=\delta_{ij}\begin{cases}|p_i|h\,\mathrm{csch}|p_i|h, & p_i^2\geqslant 0\\ |p_i|h\csc|p_i|h, & p_i^2\leqslant 0\end{cases}, \tag{37}$$

where $p_i^2=W_{ii}(x_m)$. An identical equation applies to the (m,b) half-interval propagators in Eq. (31).

Also, Alexander and Manolopoulos[30] have presented an alternative, "potential following,"[25] log-derivative propagation scheme, valid in the regime where the potential is more slowly varying than the wave function. In this case the coupled equations are diagonalized at the midpoint x_m of the interval,[18,25,28,30,33] and the $\mathbf{W}$ matrix in this locally adiabatic basis approximated by

$$[\mathbf{W}(x)]_{ij}\cong\delta_{ij}[W_i^0+(x-x_m)W_i^1]. \tag{38}$$

The log-derivative propagators for the (a,b) interval can then be expressed in terms of the Airy functions[35] $\mathrm{Ai}(u)$ and $\mathrm{Bi}(u)$ in the variable $u_i=\alpha_i(x+\beta_i)$, where $\alpha_i=(W_i^1)^{1/3}$ and $\beta_i=(W_i^0-x_mW_i^1)/W_i^1$. In this linear reference potential implementation, the full-interval propagators, $\mathbf{L}_i(a,b)$, in Eqs. (25)–(27) are diagonal with the diagonal elements given by

$$[\mathbf{L}_1(a,b)]_{ii}=\alpha[\mathrm{Ai}(u_{i2})Bi'(u_{i1})-\mathrm{Ai}'(u_{i1})\mathrm{Bi}(u_{i2})]/D_i(a,b), \tag{39a}$$

$$[\mathbf{L}_2(a,b)]_{ii}=[\mathbf{L}_3(a,b)]_{ii}=\alpha/[\pi D_i(a,b)], \tag{39b}$$

$$[\mathbf{L}_4(a,b)]_{ii} = \alpha[\mathrm{Ai}(u_{i1})\mathrm{Bi}'(u_{i2}) - \mathrm{Ai}'(u_{i2})\mathrm{Bi}(u_{i1})]/D_i(a,b), \quad (39c)$$

where

$$u_{i1} = \alpha_i(x_a - \beta_i), u_{i2} = \alpha_i(x_b - \beta_i), \text{ and}$$
$$D_i(a,b) = \mathrm{Ai}(u_{i1})\mathrm{Bi}(u_{i2}) - \mathrm{Ai}(u_{i2})\mathrm{Bi}(u_{i1}). \quad (40)$$

We have given elsewhere[30] explicit expressions for the Airy propagators in Eqs. (39) and (40), which completely eliminate all problems of numerical stability[18,25,30,36] associated with either the exponential growth of the Airy functions at large positive argument or the oscillations at large negative argument.

IV. APPLICATIONS

As a first application of our method we chose to treat a well-studied model corresponding to the middle panel of Fig. 1, in which two linear potentials cross and are coupled by a constant, small potential. The linear potentials are defined by

$$V_{11}(x) = a_0 + a_1 x, \quad (41a)$$
$$V_{22}(x) = a_0 - a_2(x), \quad (41b)$$

The semiclassical limit for this special case has been worked out by Coveney *et al.*[5] Their expression for the transition probability [Eqs. (8) and (87) of Ref. 5], adapted to this particular case, is

$$P_{12} = [\beta^{2/3}\pi\,\mathrm{Ai}(-\beta^{2/3}\epsilon)]^2, \quad (42)$$

where

$$\epsilon = E(a_1 + a_2)/(2V_{12}\bar{a}) \quad (43)$$

and

$$\beta = 4V_{12}[\mu V_{12}/(\hbar^2\bar{a}(a_1 + a_2)]^{1/2}, \quad (44)$$

where V_{12} is the constant coupling potential, and $\bar{a} = (a_1 a_2)^{1/2}$.

The choice of the parameters was guided by our *ab initio* calculations on the decomposition of HN_3.[7-9] We took $V_{12} = 45\ \mathrm{cm}^{-1}$, $a_0 = 8900\ \mathrm{cm}^{-1}$, $a_1 = 4573.5\ \mathrm{cm}^{-1}/\mathrm{bohr}$, $a_2 = 21\,030\ \mathrm{cm}^{-1}/\mathrm{bohr}$ and $\mu = 9.7732$ amu, appropriate for the NN–NH system. Figure 2 displays the probability for transitions from state $|1\rangle$ to state $|2\rangle$ as a function of the energy, and compares the predictions of the semiclassical expression of Coveney *et al.* with the exact results, given by the log-derivative propagation technique presented here. Converged results could be obtained using ~200 intervals over the range $-3 < x < 2$ bohr. The agreement is excellent. Physically the pronounced oscillatory structure reflects, in a semiclassical model, interference between trajectories which undergo a transition from state $|1\rangle$ to $|2\rangle$ while moving from right to left, and those which first bounce off the repulsive wall of state $|1\rangle$ before undergoing this transition.

In order to investigate the situation described in the right-hand panel of Fig. 1, in which state $|1\rangle$ is closed as $x \to \infty$ at low energy but becomes open at higher energy, we have used two diabatic potentials defined by (with energies in cm^{-1} and distances in bohr)

$$V_{11} = 5000[1 - \tanh(x - 1)], \quad (45a)$$
$$V_{22} = 4000 + 10\,000[1 - \tanh(x - 1/2)], \quad (45b)$$

and

$$V_{12} = 22.5\{1 + \tanh[2(x + 1)]\}, \quad (46)$$

which are displayed in Fig. 3. The adiabatic barrier for this system is 8892 cm^{-1} high and occurs at $x = -0.052$ bohr. The threshold for the opening of state $|1\rangle$ is 10 000 cm^{-1}. As in the calculation illustrated in Fig. 1, we have taken the reduced mass to be 9.7732 amu.

The outgoing flux in state $|2\rangle$ at energies below the

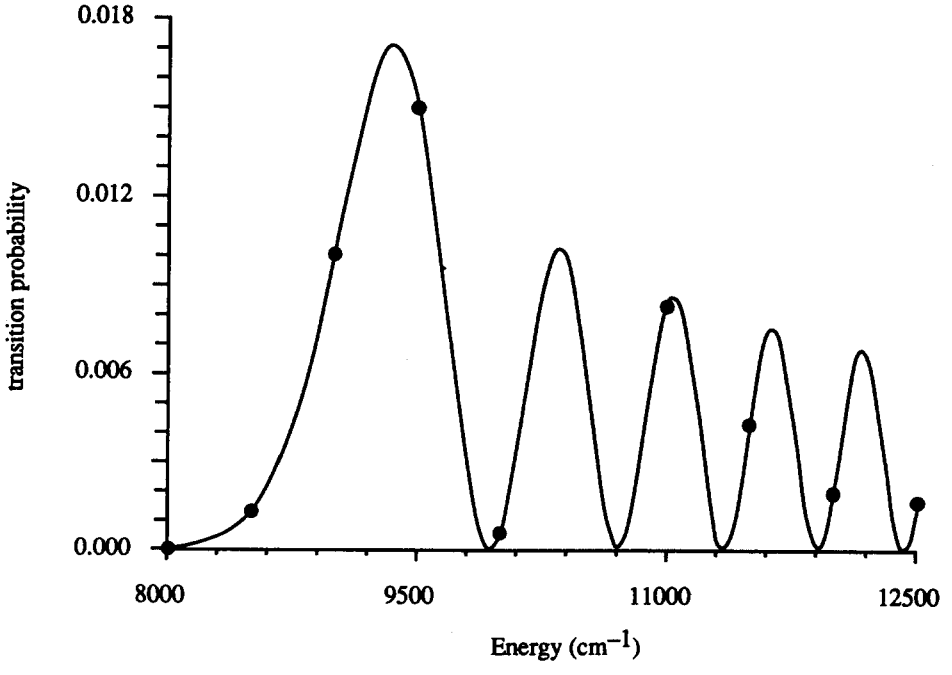

FIG. 2. Transition probability as a function of the energy for the two-state model with linear potential and constant coupling. The parameters are defined in Eq. (41) of Sec. IV. The solid curve indicates the values predicted from the semiclassical expression of Coveney *et al.* [Eq. (42) and Ref. 5], while the solid circles are the exact quantum values calculated using the log-derivative method described here.

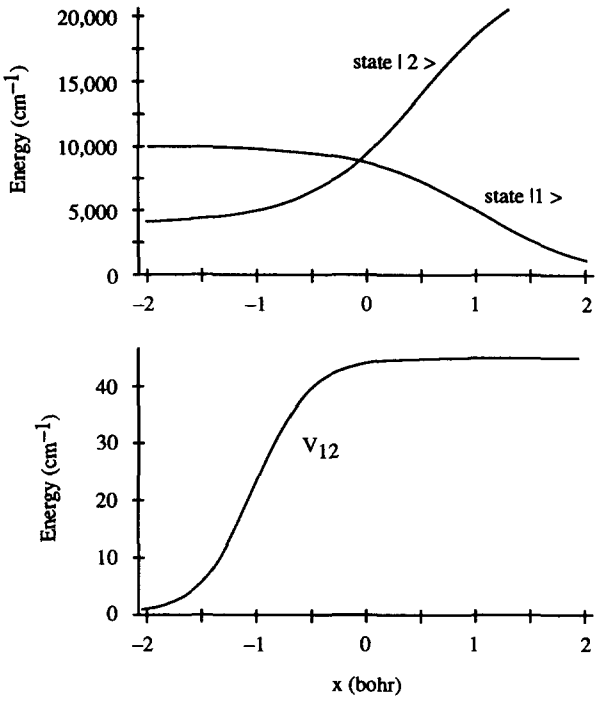

FIG. 3. (Upper panel) Diabatic potentials for the model two-state problem corresponding to the righ-hand panel in Fig. 1. The equations for the two curves are given by Eq. (45). (Lower panel) Coupling potential [Eq. (46)] for the two-state problem defined in the upper panel.

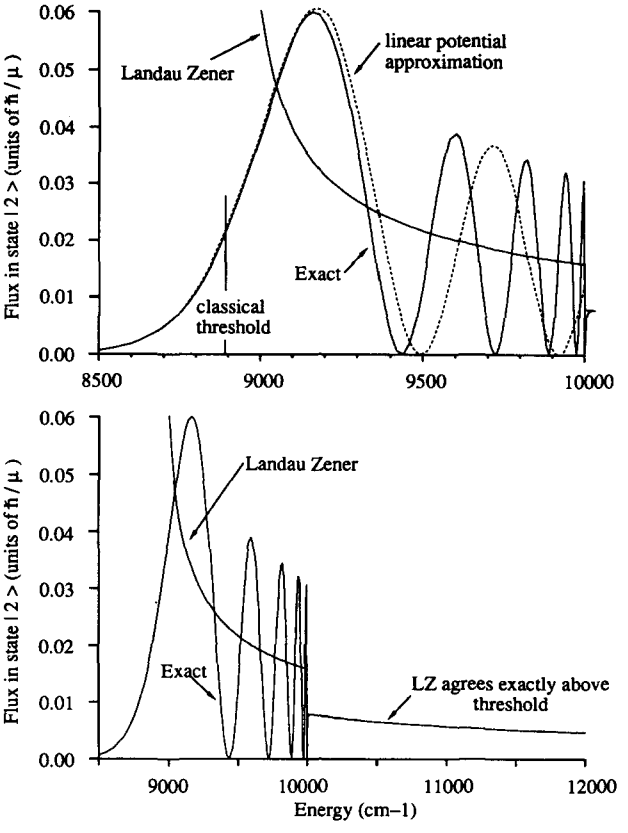

FIG. 4. Transmitted ($x \to -\infty$) flux corresponding to an incoming wave of unit flux in state $|1\rangle$ as a function of the energy for the two-state model defined in the Fig. 3. (Upper panel) Flux into state $|2\rangle$ at energies below (and just above) the threshold for state $|1\rangle$. The solid curve is the exact result calculated using the log-derivative method described here while the dashed curve indicates the values predicted from the semiclassical expression of Coveney *et al.* [Eq. (42) and Ref. 5], based on the values of the coupling potential and the derivatives of the diabatic potentials evaluated at the crossing point. Also indicated are the predictions of the classical Landau–Zener predictions [Eq. (47)]. (Lower panel) Outgoing flux as a function of the energy for $|1\rangle \to |2\rangle$ transitions at energies both above and below the threshold for state $|1\rangle$. The Landau–Zener and exact results agree extremely well above the threshold for state $|1\rangle$.

threshold for state $|1\rangle$ is shown in the upper panel of Fig. 4. For comparison, we have indicated by a dashed curve the results predicted by the semiclassical linear model result of Coveney *et al.* [Eq. (42)], where the derivatives are taken to be those of the potentials defined by Eq. (45) evaluated at the point of crossing ($x = -0.052$ bohr). A constant coupling of 45 cm^{-1} was assumed. The exact and semiclassical results agree closely at low energy, but differ substantially at higher energies, as the deviation from linear behavior becomes larger (Fig. 3).

For comparison we have also plotted the triplet flux predicted by the standard Landau–Zener formula,[1] namely

$$P_{12} = 2[1 - \exp(-\pi\zeta/4)]. \tag{47}$$

Here

$$\zeta = 8V_{12}^2 \Big/ \left[\hbar v \frac{\partial |(V_{11} - V_{22})|}{\partial x}\right], \tag{48}$$

where $v = (2E/\mu)^{1/2}$ is the relative velocity and the derivative is evaluated at the point of crossing. The factor of 2 in Eq. (47) reflects the fact that a transition from state $|1\rangle$ to $|2\rangle$ can occur while as the system moves from right to left, or, subsequently, after the system bounces off the repulsive wall of state $|1\rangle$ and then moves from left to right through the crossing. Since the transition probability is small, it is not necessary to consider further reflections. Above the threshold for state $|1\rangle$, however, this factor of two must be eliminated. As expected, the Landau–Zener probability is too large just above threshold,[2(b)] and does not, of course, contain the quantum interference effects. In an average sense, the Landau–Zener prediction is quite good. Above the threshold for state $|1\rangle$, where there are no further interferences, the Landau–Zener prediction is near quantitative.

As a measure of the accuracy of the log-derivative propagation technique presented here, Fig. 5 displays the relative error in the calculated flux for transitions from state $|1\rangle$ to both state $|2\rangle$ and state $|1\rangle$ at several energies, as a function of the number of intervals used. In all cases the range of integration was $-3 \leqslant x \leqslant +3$. The potential and parameters were identical to those used to determine the fluxes in Fig. 4. As can be seen, convergence is rapid, especially when (lower panel) the reference half-interval propagators, $\mathbf{L}_i^0(q,p)$, of Manolopoulos[29,33] are used. The error in a "solution-following" log-derivative propagation scheme is expected to be $O(h^4)$,[27,33] where h is the interval size. This high-order convergence is seen clearly in Fig. 5.

V. CONCLUSIONS

We have presented here an application of log-derivative propagators to the solution of electronic state curve crossing

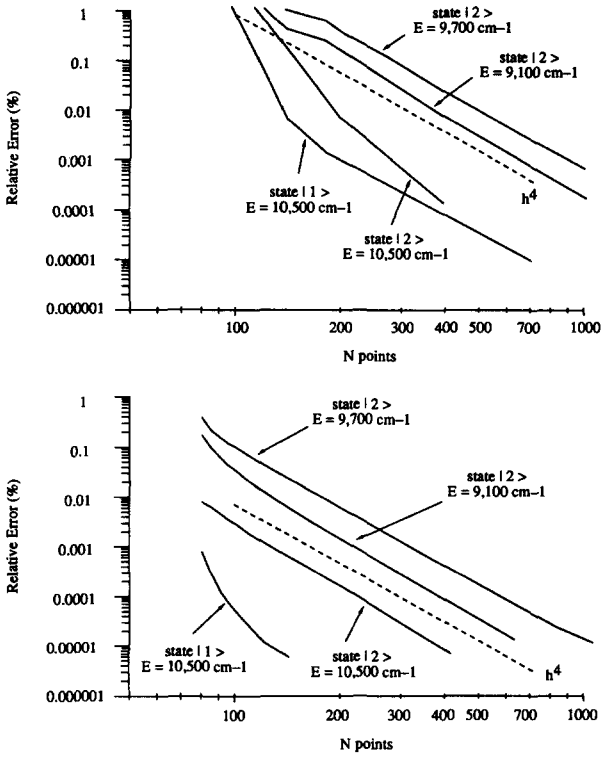

FIG. 5. Relative error in the calculated fluxes for transitions from state $|1\rangle$ to both state $|2\rangle$ and state $|1\rangle$ at several energies, as a function of the number of intervals used. In all cases the integration range was $-3 \leqslant x \leqslant +3$. The potential and parameters were identical to those used to determine the fluxes in Fig. 4. (Upper panel) Results obtained taking the reference half-interval propagators, $\mathbf{L}_i^0(q,p)$ in Eqs. (29) and (31), multiplied by the half-interval step size h, to be equal to a unit matrix, consistent with the original log-derivative algorithm of Johnson.[21,33] (Lower panel) Results obtained using the reference half-interval propagators of Manolopoulos[29,33] [Eqs. (36)].

problems. The technique is similar to work presented earlier by Mrugala and Secrest[32] for solution of collinear reactive scattering problems. In contrast to the usual implementation of log-derivative propagation techniques to inelastic collision problems,[21,27,29,30,33] it is here necessary to propagate through the range of integration not only the log-derivative matrix itself but also a transformation matrix, which permits one to recover the initial asymptotic wave function from the asymptotic wave function at the end of the integration range. Although the formal development and applications were limited here to a one-dimensional problem, the extension to one (or more) internal degrees of freedom is straightforward. The method is completely general, independent of the number of states open at either end of the range of integration; extremely simple to apply; and both rapidly convergent and numerically stable, eliminating the need for the use of stabilizing transformations[18] when propagating into a classically forbidden region. In comparison with the standard log-derivative propagation algorithm,[21,29,30,33] implementation of the method presented here requires an additional computational overhead of only two matrix multiplications per interval [one in Eq. (33) and the second in accumulating the product in Eq. (28)], in a "solution following" approximation, and only one matrix multiplication in the "potential following" approximation. In the latter case the matrix multiplication in Eq. (33) is eliminated, since propagation across an interval is done directly, without the intermediate propagation to the midpoint. Since matrix multiplications are the most efficient matrix operation on vector processors, this additional overhead will be small. The log-derivative propagation scheme presented here should be a useful complement to either semiclassical[2–6] or time-dependent[7,8] approaches to curve crossing problems.

ACKNOWLEDGMENTS

The research described here was supported in part by the Air Force Office of Scientific Research, Contract No. F49620-88-C-0056 and by the National Science Foundation, Grant No. CHE87-05912. M.H.A. wishes to thank Horia Metiu for stimulating discussions and David Manolopoulos for his encouragement, advice, and helpful comments.

[1] L. D. Landau, Phys. Z. Sowjetunion **2**, 46 (1932); C. Zener, Proc. R. Soc. Ser. A **137**, 696 (1932); E. C. G. Stueckelberg, Helv. Phys. Acta **5**, 369 (1932).
[2] (a) M. S. Child, *Molecular Collision Theory* (Academic, New York, 1974); (b) in *Atom-Molecule Collision Theory: A Guide for the Experimentalist,* edited by R. B. Bernstein (Plenum, New York, 1979), p. 427.
[3] B. C. Eu, *Semiclassical Theories of Molecular Scattering* (Springer, Berlin, 1984).
[4] E. E. Nikitin and S. Ya. Umanskii, *Theory of Slow Atomic Collisions* (Springer, Berlin, 1984).
[5] P. V. Coveney, M. S. Child, and A. Bárány, J. Phys. B **18**, 457 (1985).
[6] H. Nakamura, J. Phys. Chem. **88**, 4812 (1984); J. Chem. Phys. **87**, 4031 (1987); in *Electronic and Atomic Collisions,* edited by H. B. Gilbody, W. R. Newell, F. H. Read, and A. C. H. Smith (Elsevier, New York, 1988), p. 413.
[7] S.-I. Sawada and H. Metiu, J. Chem. Phys. **84**, 227, 6293 (1986).
[8] J. Alvarellos and H. Metiu, J. Chem. Phys. **88**, 4957 (1988).
[9] V. Engel, H. Metiu, R. Almeida, R. A. Marcus, and A. H. Zewail, Chem. Phys Lett. **152**, 1 (1988).
[10] T. S. Rose, M. J. Rosker, and A. H. Zewail, J. Chem. Phys. **88**, 6672 (1988).
[11] M. H. Alexander, H.-J. Werner, and P. J. Dagdigian, J. Chem. Phys. **89**, 1388 (1988).
[12] M. H. Alexander and P. J. Dagdigian, Am. Inst. Phys. Conf. Proc. (to be published) (1989).
[13] M. H. Alexander, T. H. Hemmer, H.-J. Werner, and P. J. Knowles, J. Chem. Phys. (submitted).
[14] B. R. Foy, M. P. Casassa, J. C. Stephenson, and D. S. King, J. Chem. Phys. **89**, 608 (1988); J. C. Stephenson, M. P. Casassa, and D. S. King, *ibid.* **89**, 1378 (1988); B. Foy, M. P. Casassa, J. C. Stephenson, and D. S. King, *ibid.* **90**, 7037 (1989).
[15] B. R. Johnson and D. Secrest, J. Math. Phys. **7**, 2187 (1966).
[16] P. Pechukas and J. C. Light, J. Chem. Phys. **44**, 3897 (1966); D. Chang and J. C. Light, *ibid.* **50**, 2517 (1969).
[17] W. A. Lester, Jr., J. Comput. Phys. **3**, 322 (1968); Meth. Comput. Phys. **10**, 211 (1971).
[18] R. G. Gordon, J. Chem. Phys. **51**, 41 (1969); Meth. Comput. Phys. **10**, 81 (1971).
[19] W. N. Sams and D. J. Kouri, J. Chem. Phys. **51**, 4809 (1969).
[20] A. C. Allison, J. Comput. Phys. **6**, 378 (1970).
[21] B. R. Johnson, J. Comput. Phys. **13**, 445 (1973).
[22] M. J. Redmon and D. A. Micha, Chem. Phys. Lett. **28**, 341 (1974).
[23] J. C. Light and R. B. Walker, J. Chem. Phys. **65**, 4272 (1976); E. B. Stechel, R. B. Walker, and J. C. Light, *ibid.* **69**, 3518 (1978); G. A. Parker, T. G. Schmalz, and J. C. Light, *ibid.* **73**, 1757 (1980).
[24] B. R. Johnson, J. Chem. Phys. **69**, 4678 (1978).
[25] D. Secrest, in *Atom-Molecule Collision Theory: A Guide for the Experimentalist,* edited by R. B. Bernstein (Plenum, New York, 1979), p. 265.
[26] P. L. DeVries and T. F. George, Mol. Phys. **39**, 701 (1980).
[27] L. D. Thomas, M. H. Alexander, B. R. Johnson, W. A. Lester, Jr., J. C. Light, K. D. McLenithan, G. A. Parker, M. J. Redmon, T. G. Schmalz,

D. Secrest, and R. B. Walker, J. Comput. Phys. **41**, 407 (1981).
[28]M. H. Alexander, J. Chem. Phys. **81**, 4510 (1984).
[29]D. E. Manolopoulos, J. Chem. Phys. **85**, 6425 (1986).
[30]M. H. Alexander and D. E. Manolopoulos, J. Chem. Phys. **86**, 2044 (1987).
[31]F. Mrugala and D. Secrest, J. Chem. Phys. **78**, 5954 (1983).
[32]F. Mrugala and D. Secrest, J. Chem. Phys. **79**, 5960 (1983).
[33]D. Manolopoulos, thesis, University of Cambride (UK), 1988.
[34]M. H. Alexander and B. Pouilly, J. Chem. Phys **90**, 5373 (1989).
[35]M. Abramowitz and I. Stegun, Natl. Bur. Stand. Appl. Math. Ser. **55** (1965), Sec. 10.3.
[36]J. Canosa and R. G. de Olivera, J. Comput. Phys. **5**, 188 (1970).